

Polarized red and blue light emission from silicon-based nanostructures correlated with crystallographic axes

B. Goller and D. Kovalev*

Department of Physics, University of Bath, Bath BA2 7AY, United Kingdom

(Received 9 March 2011; published 27 June 2011)

Energy-selective photoluminescence spectroscopy of porous silicon has been used to study the morphology of porous silicon layers prepared from (110) silicon wafers. We demonstrate that the electric field vector of the red emission band is aligned along the principal crystallographic axes of bulk silicon. From these observations, we conclude that large and small silicon nanocrystals assembling the layers have different preferential crystallographic orientations. Oxidized porous silicon layers exhibit a blue emission band which is strongly polarized along the $\langle 100 \rangle$ crystallographic axes. This indicates that chain-like silicon clusters, preferentially aligned along the same crystallographic directions, are responsible for the blue emission.

DOI: [10.1103/PhysRevB.83.233303](https://doi.org/10.1103/PhysRevB.83.233303)

PACS number(s): 78.67.Bf, 78.66.Db, 79.60.Bm, 79.60.Jv

Measurement of the polarization of the photoluminescence (PL) is a powerful tool for investigation of the electronic symmetry of the absorbing and luminescent states as well as energy relaxation processes.¹ The excitation of the PL by polarized light can select certain optical transitions between spin-, angular momentum-, or linear momentum-degenerated states of different systems.¹ Bulk silicon (Si) has a cubic lattice structure and to observe a polarized PL from Si either an external perturbation which lifts the hole band/valley degeneracy^{2,3} or direct spin injection⁴ is required.

The phenomenon, when a certain substance excited by linearly polarized light emits light which is also linearly polarized, is called polarization memory (PM) effect. The PM value is usually expressed as $\rho = (I_{\parallel} - I_{\perp}) / (I_{\parallel} + I_{\perp}) \times 100\%$, where I_{\parallel} and I_{\perp} are the intensities of the PL, polarized parallel and perpendicular to the direction of the electric field (polarization) of the exciting light. For semiconductor nanostructures, besides the electronic contribution to the PL polarization, dielectric screening effects have also to be taken into account. Nanocrystal (NC) or nanowire systems usually have a strong lateral modulation of the dielectric constant (ϵ).^{5,6} Since the resulting matrix element of absorption and emission is a product of the electric field strength and the dipole moment, both contributions to the PL polarization in NCs are important.^{7,8} Bulk Si is optically highly isotropic; therefore, PL polarization is mainly defined by the local electric field inside the Si NCs/nanowires.⁹⁻¹¹

PSi is usually produced via electrochemical etching of bulk Si wafers.¹² The morphology of PSi layers is found to be strongly dependent on the type of the Si wafer and anodization conditions. Due to quantum confinement effects, PSi, similar to other nanosilicon systems, exhibits size-tunable efficient red and near infrared PL.¹² One of the most interesting features of the PL from PSi is its high ρ value which cannot be understood via coherent quantum mechanical effects.⁹ The nature of absorbing and emitting dipoles has to be quite different taking into account that a photoexcited electron-hole pair loses energy of about 1–2 eV in inelastic processes and, therefore, the observed PM is not a coherent effect.

The unusual behavior of PSi PL polarization has been attributed to the nonsphericity of Si NCs and to a large difference in the values of ϵ of NCs and the surrounding

medium.^{9,13} Indeed, we found that the PL from spherical Si NCs is not polarized. Since the size of NCs assembling PSi is much smaller than the wavelength of the exciting light, this problem can be solved in electrostatic terms.^{9,13} The electric field of light induces polarization charges at the surface of NCs which decrease the strength of the electric field inside them. The effect is weaker when the electric field is applied along the longer dimension of Si NCs. The probability of optical absorptions and emission is proportional to the square of the electric field inside the NC and, therefore, NCs whose longest dimensions are aligned along the polarization direction of the exciting light will preferentially absorb and emit photons. The resulting PL from an ensemble of randomly oriented NCs becomes predominantly polarized along the direction of the polarization of the exciting light. The isotropic angular distribution of the ρ values in the (100) surface plane implies a random distribution of the NCs shapes and orientations in this plane.⁹

The situation is, however, quite different for PSi layers grown from low symmetry (110) Si wafers. They have three equivalent $\langle 100 \rangle$ axes: [001] lies in the plane of the layer while another two [100] and [010] are tilted at 45° to the (110) surface. The projection of these two axes to the surface plane of the layer coincides with the $[1\bar{1}0]$ crystallographic direction. These three axes are not in-plane equivalent and (110) PSi layers become highly optically anisotropic (form birefringence arising from preferential pore orientation).^{14,15}

PSi layers consist of an almost infinite number of Si NCs having different size, shape, and orientation. Therefore, anisotropy of ϵ is an average characteristic of PSi NC assemblies. However, morphology of PSi layers can be investigated by using PL polarization-resolved measurements. Selecting detection energy within the red emission band, different sizes of NCs can be probed while measurement of the polarization of the emitted light gives direct information about their preferential alignment. Thus, these experiments give important information on the overall structural morphology of spatially anisotropic Si NC assemblies. We found that preferential orientation of NCs assembling PSi layers is strongly size-dependent and follows the crystallographic axes of bulk Si. We demonstrate that oxidized porous silicon layers exhibit blue emission band which is also strongly polarized along

the (100) crystallographic axes. Thus, this emission originates from Si-based nanostructures and not from point defects as it was suggested before. We argue that chain-like silicon clusters preferentially aligned along these crystallographic directions are responsible for the blue emission from PSi.

In-plane anisotropy of p^- PSi, prepared from weakly doped (110) Si substrates, is smaller than for p^{++} PSi, prepared from heavily doped (110) Si substrates. For p^- PSi layers, containing small NCs (3–7 nm), the largest ϵ value is measured for light polarized along the [001] crystallographic direction,¹⁴ while for p^{++} PSi (NCs size of 10–20 nm), it is larger for the [1 $\bar{1}$ 0] crystallographic direction.¹⁵ Therefore, for our studies, we used p^- and p^{++} PSi layers prepared from boron-doped Si substrates with specified resistivity of 10 Ω cm and 10 m Ω cm, respectively. The etching solution was a 1:1 by volume mixture of hydrofluoric acid 49 wt% in water and ethanol, yielding a fully H-terminated surface. The etch current density was 50 mA/cm². Some p^{++} PSi samples were oxidized in ambient at 900 °C; after oxidation, the Si NCs are either surrounded by a SiO₂ shell or are fully oxidized. The PL was excited either by using the 488-nm line of an Ar* or by 325-nm line of a He-Cd lasers polarized by a Glan polarizer. Two PL components polarized parallel and perpendicular to that of the exciting light have been measured and, rotating the sample, angular dependencies of the PL ρ values have been measured. All measurements were performed at 300 K.

The PL of (110) p^- PSi is shown in Fig. 1 by a dashed line. Its large spectral width is due to the wide distribution of Si NCs sizes and shapes. The solid line shows the spectral dependence of the PL ρ value which is very similar to that measured for PSi prepared from (100) Si wafers.⁹ However, while for (100) PSi the ρ value does not depend on the in-plane polarization of the exciting light, due to overall alignment of Si NCs along the [100] growth direction and their random distribution in the (100) plane.^{9,12} For (110) p^- PSi layers, a well-defined anisotropy of the ρ value can be seen (inset of Fig. 1). For low detection energies (larger NCs), its maximum value is achieved when the polarization of the exciting light coincides with the [001] crystallographic direction. Therefore, large NCs are mainly aligned along in-plane [001] direction. These

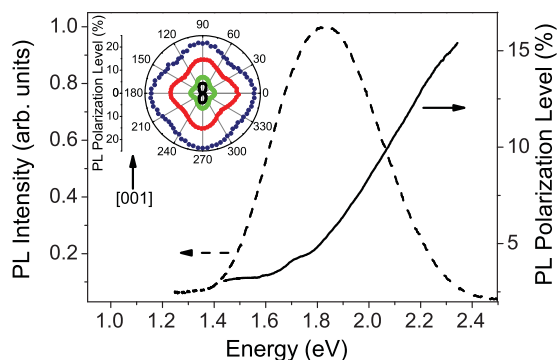


FIG. 1. (Color online) Spectral dependencies of PL intensity of (110) p^- PSi (dashed line) and the ρ value (solid line) when exciting light is polarized along the [001] direction. (Inset) Angular dependencies of the ρ value. $E_{\text{ex}} = 2.54$ eV. Detection energies, from outside to center: 2.25 eV (blue), 2.0 eV (red), 1.65 eV (green), and 1.46 eV (black).

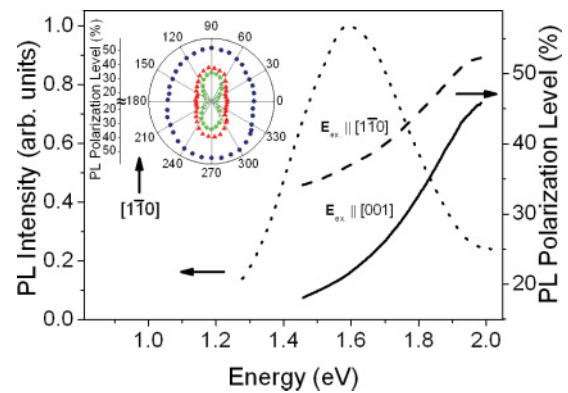


FIG. 2. (Color online) Spectral dependencies of PL intensity of (110) p^{++} PSi (dotted line) and the ρ values (solid and dashed lines) when exciting light is polarized along the [1 $\bar{1}$ 0] or [001] crystallographic directions, respectively. (Inset) Angular dependencies of the ρ values. $E_{\text{ex}} = 3.8$ eV. Detection energies from outside to center: 2.07 eV (blue), 1.77 eV (green), and 1.55 eV (red).

experiments are in a good agreement with the observation that ϵ of p^- PSi layers is the largest for the [001] direction.¹⁴ For higher detection energies, the ρ value pattern becomes more symmetric with maxima of the ρ values for the [1 $\bar{1}$ 0] and [001] directions.

The anisotropy of the ϵ value is an average morphological characteristic of the PSi layers and spectrally resolved measurements of the ρ value can give a more detailed information on which Si NCs assembling PSi layers contribute to this effect. Results of these experiments are shown in Fig. 2. Dotted line shows the PL spectrum of PSi prepared from p^{++} Si wafers. Dashed and solid lines represent the ρ value for exciting light polarized along [1 $\bar{1}$ 0] and [001] directions. The ρ value is always larger when the exciting light is polarized along the [1 $\bar{1}$ 0] direction. The anisotropy is better pronounced for lower detection energies, i.e., for larger NCs. It is important to note that the ρ value for the exciting light polarized along [1 $\bar{1}$ 0] exceeds $\rho = 0.5$, the maximal theoretical value for randomly oriented ideal linear dipoles. This confirms that there is a preferential orientation of Si NCs along the [100] and [010] crystallographic directions. This is in agreement with the results of Ref. 15. However, the spectral dependence of the ρ value can not be explained solely on the basis of dielectric model^{6,9,13} which neglects the sensitivity of the exciton wavefunctions to the shape of Si NCs. This is only true for large NCs when their size exceeds the exciton Bohr radius. For small Si nanostructures, this should not be the case. For instance, in the limit of Si chain structures, polysilanes, the symmetry (linear dipole structure) of exciton wavefunction alone results in a very high value of ρ .¹⁶ We believe that with a decrease in Si NCs size, the exciton wavefunctions become more sensitive to the shape of NCs and both effects contribute to the PM effect. This can explain the monotonous increase of the ρ value toward higher detection energy despite of a reduced level of anisotropy of nonspherical Si NCs alignment (see Fig. 2).

It is well known that successive oxidation of Si NCs assembling PSi layers results in appearance of near ultraviolet-blue PL band having a nanosecond lifetime.¹⁷ After complete

oxidation of Si NCs, PSi is transformed into porous amorphous SiO₂ which does not exhibit discernible silicon crystal structures. This material emits only this type of PL.¹² It is important to note that bulk amorphous SiO₂ exhibits similar PL spectra and lifetime.¹⁸ In many papers, this PL band was attributed to point defects in amorphous porous SiO₂ or SiO_x for instance such as a nonbridging oxygen hole centers.¹⁹

However, there is a fundamental difference in light emission properties of bulk amorphous SiO₂ and heavily oxidized PSi. Despite almost identical energy and lifetime, PL from amorphous SiO₂ does not show any PM effect while for partially or fully oxidized PSi the value of ρ can be as high as 30%.²⁰ For (100) porous SiO₂ layers, it has been found that, similar to the red emission band, its value does not depend on the in-plane direction of the polarization of the exciting light. Thus, the nature of light emitters in fused silica and heavily oxidized PSi should be different.

To clarify the origin of the blue PL band, we performed comparative studies of the polarization properties of the red and blue PL band, exhibited by partially oxidized p^{++} PSi layers (see Fig. 3). The dotted line shows a PL spectrum, containing a red emission band having identical PL properties as nonoxidized PSi layers and a near ultraviolet-blue band with a maximum PL emission at 2.8 eV. Both PL bands exhibit high ρ values. The ρ value of the red PL band for oxidized samples is much smaller than that for as-prepared ones due to SiO₂ formation and, therefore, a reduced dielectric mismatch. For the red emission band the value of ρ , similar to nonoxidized PSi layers, is larger when the exciting light is polarized along the $[1\bar{1}0]$ direction while for the blue band $[1\bar{1}0]$ and $[001]$ directions are found to be almost equivalent.

The inset of Fig. 3 shows the angular dependence of the ρ value for partially oxidized p^{++} PSi layers. For low detection energies (red PL band), the angular dependence of the ρ value is almost identical to that shown in Fig. 2, ρ is maximal for the $[1\bar{1}0]$ direction. However, at higher detection energies (for smaller NCs), the second distinct in-plane $[001]$ axis of Si NC alignment becomes prominent. Since according to Ref. 21, the thermal oxidation rates of crystalline Si along the $\langle 110 \rangle$ and

$\langle 111 \rangle$ directions are higher than that along the $\langle 100 \rangle$ directions, thermal oxidation can completely modify the morphology of PSi layers. This can be seen in the angular dependencies of the ρ values for as-prepared and partially oxidized p^{++} PSi layers (compare insets of Figs. 2 and 3). Anisotropy of the oxidation process results in the formation of an additional fraction of Si NCs preferentially aligned along the $[001]$ direction and this effect should be stronger for smaller NCs. This is confirmed by the experiments shown in the inset of Fig. 3.

The ρ values for the blue band for $[1\bar{1}0]$ and $[001]$ directions are found to be almost equal, but slightly higher for the exciting light polarized parallel to the $[001]$ direction. Since projections of the $[100]$ and $[010]$ axes on the (110) surface coincide with the $[1\bar{1}0]$ direction, the blue band is preferentially polarized in equivalent $\langle 100 \rangle$ directions. It also implies that the intensity of the PL polarized along these directions is almost identical. It is important to mention that we performed similar experiments for samples which are regarded in the literature as “fully oxidized PSi.” They exhibit only the blue PL band and we found that the angular dependence of the ρ value is identical to that shown in Fig. 3 at a detection energy of 2.8 eV. In these samples, Si NCs do not exist and, therefore, emitting states cannot be associated with their surface. It is believed that this material is amorphous porous quartz; however, the observed strong PL polarization anisotropy, which correlates with the crystalline axes of Si, evidences a structural order responsible for the blue emission. The observation that the ρ value anisotropy of the blue band coincides with the principle crystallographic axes of bulk Si, to our opinion, rules out point defects as a source for the blue PL emission from oxidized PSi. Indeed, neither absorption nor emission of point defects, such as in amorphous SiO₂, should be sensitive to the direction of the electric field of the exiting light. The dielectric model cannot explain this anisotropy as well: ϵ of SiO₂ is very small compared to Si while the ρ value for the blue band is much higher than that of the red PL band of the same sample. The well-defined anisotropy of the ρ value indicates that the remaining Si-based nanostructures are responsible for the blue emission.

Optical studies of clusters and wires containing from a few to many atoms help to understand how molecules evolve into solids or how, with progressive size reduction, solids can evolve in molecular-like structures. It has been demonstrated that for the smallest Si NCs, when the notion “unit crystal cell” still can be applied, the PL is in the green range and exciton lifetime is still in microsecond time domain.¹² On the other hand, chain-like Si-based polymer molecules (polysilanes) have identical PL properties to the blue emission of heavily oxidized PSi: they exhibit a similar PL energy and lifetime and a high PM level.¹⁶ Polysilane molecules imbedded in silica demonstrate also almost identical optical properties.²² Since the polarization properties of the red and blue PL from (110) PSi layers correlate with the crystalline axes of bulk Si, we believe that both PL bands are related to Si nanostructures. It is obvious that the angular polarization pattern of the red PL band is related to the preferential alignment of Si NCs along certain crystallographic directions of Si wafers,^{9,15} this is confirmed by high resolution transmission electron microscopy.^{12,15} Oxidation of Si NCs which are aligned along equivalent $\langle 100 \rangle$ directions can finally result in the formation of molecular-like

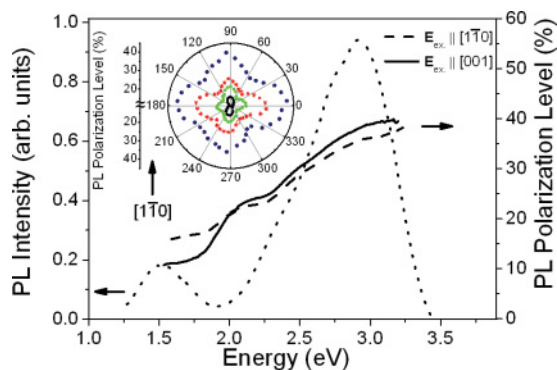


FIG. 3. (Color online) Spectral dependencies of PL intensity for the partially oxidized (110) p^{++} PSi (dotted line) and the ρ values (solid and dashed lines) when the exciting light is polarized along the $[001]$ or $[1\bar{1}0]$ crystallographic directions, respectively. (Inset) Angular dependencies of the ρ values. $E_{\text{ex}} = 3.8$ eV. Detection energies from outside to center: 2.8 eV (blue), 2.34 eV (red), 1.9 eV (green), and 1.55 eV (black).

Si chain structures, similar to polysilanes, aligned along the same crystallographic directions. The angular dependence of the ρ value strongly supports this conjecture. For this type of Si-based nanostructures, classical quantum confinement arguments are not valid and their emission properties should be completely different from those of Si NCs (the ρ value, PL energy, and lifetime). To our opinion, the observed angular dependence of the ρ value strongly supports this idea.

To conclude, we have shown that spectrally-resolved PL PM measurements are a powerful tool to investigate the

size-dependent morphology of spatially anisotropic Si nanostructures. They give valuable information about the general alignment of Si nanostructures assembling PSi layers. We demonstrated that there is a certain alignment of Si NCs along the $\langle 100 \rangle$ crystal axes and its level depends on the conductivity of the Si substrates used. We also argue that chain-like Si nanostructures, imbedded in amorphous SiO₂ and aligned along the principle $\langle 100 \rangle$ axes of bulk Si, are responsible for the blue PL emission from oxidized PSi layers. This approach can be useful for the identification of the morphology of other nanostructured systems.

*d.kovalev@bath.ac.uk

¹*Optical Orientation, Modern Problems in Condensed Matter Sciences*, edited by F. Meier and B. P. Zakharchenya (North-Holland Publ. Co., Amsterdam, 1984).

²H. A. Lorentz, *Collected Papers*, Vol. II (Nijhoff, Dordrecht, The Netherlands, 1936), p. 79.

³N. V. Alkeev, A. S. Kaminskii, and Ya. E. Pokrovskii, *Fiz. Tverd. Tela* **18**, 713 (1976).

⁴B. T. Jonker, G. Kioseoglou, A. T. Hanbicki, C. H. Li, and P. E. Thompson, *Nat. Phys.* **3**, 542 (2007).

⁵P. Ils, C. Greus, A. Forchel, V. D. Kulakovskii, N. A. Gippius, and S. G. Tikhodeev, *Phys. Rev. B* **51**, 4272 (1995).

⁶H. E. Ruda and A. Shik, *Phys. Rev. B* **72**, 115308 (2005).

⁷D. Kovalev, M. Ben-Chorin, J. Diener, B. Averboukh, G. Polisski, and F. Koch, *Phys. Rev. Lett.* **79**, 119 (1997).

⁸T. B. Hoang, A. F. Moses, L. Ahtapodov, H. Zhou, D. L. Dheeraj, A. T. J. van Helvoort, B. Fimland, and H. Weman, *Nano Lett.* **10**, 2927 (2010).

⁹D. Kovalev, M. Ben Chorin, J. Diener, F. Koch, Al. L. Efros, M. Rosen, N. A. Gippius, and S. G. Tikhodeev, *Appl. Phys. Lett.* **67**, 1585 (1995).

¹⁰J. Wang, M. S. Gudiksen, X. Duan, Y. Cui, and C. M. Lieber, *Science* **293**, 1455 (2001).

¹¹B. Bruhn, J. Valenta, and J. Linnros, *Nanotechnology* **20**, 505301 (2009).

¹²A. G. Cullis, L. T. Canham, and P. D. J. Calcott, *J. Appl. Phys.* **82**, 909 (1997) and references therein.

¹³P. Lavallard and R. A. Suris, *Solid State Commun.* **25**, 267 (1995).

¹⁴D. Kovalev, G. Polisski, J. Diener, H. Heckler, N. Künzner, V. Yu. Timoshenko, and F. Koch, *Appl. Phys. Lett.* **78**, 916 (2001).

¹⁵N. Künzner, D. Kovalev, J. Diener, E. Gross, V. Yu. Timoshenko, G. Polisski, F. Koch, and M. Fujii, *Opt. Lett.* **26**, 1265 (2001).

¹⁶Y. Kanemitsu, *Phys. Rep.* **263**, 1 (1995), and reference therein.

¹⁷D. I. Kovalev, I. D. Yaroshetzki, T. Muschik, V. Petrova-Koch, and F. Koch, *Appl. Phys. Lett.* **64**, 214 (1994).

¹⁸J. H. Stathis and M. A. Kastner, *Phys. Rev. B* **35**, 2972 (1987).

¹⁹L. Tsybeskov, J. V. Vandyshev, and P. M. Fauchet, *Phys. Rev. B* **49**, 7821 (1994).

²⁰A. V. Andrianov, D. I. Kovalev, N. N. Zinovè, and I. D. Yaroshetskii, *JETP Lett.* **58**, 417 (1993).

²¹E. A. Irene, H. Z. Massoud, and E. Tierney, *J. Electrochem. Soc.* **133**, 1253 (1986).

²²A. Kobayashi, H. Naito, Y. Matsuura, K. Matsukawa, H. Inoue, and Y. Kanemitsu, *Jpn. J. Appl. Phys.* **41**, L1467 (2002).